Title

Nanotoxoid vaccination protects against opportunistic bacterial infections arising from immunodeficiency

Journal

Science Advances, 8(36)

ISSN

2375-2548

Authors

Zhou, Jiarong

Krishnan, Nishta

Guo, Zhongyuan

et al.

Publication Date

2022-09-09

DOI

10.1126/sciadv.abq5492

IMMUNOLOGY

Nanotoxoid vaccination protects against opportunistic bacterial infections arising from immunodeficiency

Jiarong Zhou, Nishta Krishnan, Zhongyuan Guo, Christian J. Ventura, Maya Holay, Qiangzhe Zhang, Xiaoli Wei, Weiwei Gao, Ronnie H. Fang*, Liangfang Zhang*

The rise in nosocomial infections caused by multidrug-resistant pathogens is a major public health concern. Patients taking immunosuppressants or chemotherapeutics are naturally more susceptible to infections. Thus, strategies for protecting immunodeficient individuals from infections are of great importance. Here, we investigate the effectiveness of a biomimetic nanotoxoid vaccine in defending animals with immunodeficiency against *Pseudomonas aeruginosa*. The nanotoxoids use a macrophage membrane coating to sequester and safely present bacterial virulence factors that would otherwise be too toxic to administer. Vaccination with the nanoformulation results in rapid and long-lasting immunity, protecting against lethal infections despite severe immunodeficiency. The nanovaccine can be administered through multiple routes and is effective in both pneumonia and septicemia models of infection. Mechanistically, protection is mediated by neutrophils and pathogen-specific antibodies. Overall, nanotoxoid vaccination is an attractive strategy to protect vulnerable patients and could help to mitigate the threat posed by antibiotic-resistant superbugs.

INTRODUCTION

The rise of antibiotic-resistant bacteria is a serious threat to global health with potentially devastating consequences (*1*, *2*). As superbugs continue to evolve and develop resistance while the discovery of new drugs remains stagnant, it is apparent that traditional antibiotic-based therapeutic approaches for treating bacteria will become increasingly inadequate (*3*). Infections caused by antibiotic-resistant pathogens are most prevalent in hospital settings, largely due to comorbidities and complications resulting from treatments (*4*, *5*). In particular, patients with compromised immune systems are more susceptible to infections, allowing opportunistic pathogens to invade and proliferate with little restraint (*6*–*8*). This can occur when patients are taking immunosuppressants for hematopoietic stem cell transplants (*9*), graft-versus-host diseases (GVHD) (*10*), autoimmune disorders (*11*), and other inflammatory conditions (*12*). Patients who are infected with human immunodeficiency virus (*13*), undergoing chemotherapy (*14*), or prescribed specific classes of medications such as interferons (*15*), certain antibiotics (*16*, *17*), and antidepressants (*18*, *19*) can likewise become immunodeficient. Hence, to control the spread of antibiotic resistance, the development of solutions for protecting these vulnerable patient populations is critical.

An emerging strategy for combatting antibiotic-resistant pathogens is antivirulence vaccination using nanotoxoids (*20*, *21*). During infections, bacteria can secrete a plethora of virulence factors to assist with colonization. While these toxic secretions are attractive targets for vaccine development, effective strategies for enhancing their safety without compromising immunogenicity and antigenicity are required. As they must engage with the plasma membrane of target cells to exert their activity, bacterial toxins can be captured and inactivated by biomimetic nanoparticles wrapped in naturally derived host cell membrane (*22*). Nanotoxoids are constructed by leveraging cell membrane–coated nanoparticles to sequester virulence factors in their native forms, enabling the resulting complex to be used as a vaccine for safely eliciting antibacterial immunity (*21*). Since their immunocompatible cell membrane coating confers broad neutralization capabilities, nanotoxoids targeting multiple antigens can be readily fabricated from undefined bacterial secretions. This strategy has been successfully applied against methicillin-resistant *Staphylococcus aureus* and *P. aeruginosa* (*23*, *24*); both bacteria belong to the list of ESKAPE pathogens that are considered highly virulent and resistant to antibiotics (*25*), and the World Health Organization has designated *P. aeruginosa* as one of three multidrug-resistant pathogens for which there is the most pressing need for novel antibiotics (*26*). *P. aeruginosa* is an opportunistic pathogen and is the most common Gram-negative bacteria responsible for nosocomial infections (*27*). Treatment options for multidrug-resistant *P. aeruginosa* are limited (*28*, *29*). Many experimental vaccines have demonstrated potential, but none have been clinically approved (*30*–*34*).

Here, we evaluated a macrophage membrane-coated nanotoxoid (MΦ-NT) vaccine against *P. aeruginosa* in a clinically relevant murine model of immunodeficiency induced by the DNA-alkylating agent cyclophosphamide (CP), a commonly used chemotherapeutic and immunosuppressant drug that has leukodepletive effects (*35*). Without vaccination, leukodepleted mice were highly susceptible to *P. aeruginosa* invasion due to their compromised immune systems, whereas animals receiving MΦ-NT before the induction of immunodeficiency were protected to the same degree as fully immunocompetent mice that were also administered the nanotoxoid vaccine (Fig. 1A). Efficacy was assessed in pneumonia and septicemia models of bacterial infection, and significant protection was achieved using both subcutaneous and intranasal routes of immunization. Mechanistically, neutrophils along with the presence of antibodies specific to *P. aeruginosa* were identified as major contributors to the reduction in bacterial burden. Upon vaccination with a modest dose of MΦ-NT, mice rapidly developed immunity that lasted for a minimum of 4 months. In addition, in a model of age-related immunodeficiency, elderly mice 72 weeks in age that received MΦ-NT were able to resist infection as well as young, vaccinated mice. Last, it was also demonstrated that MΦ-NT could be

Department of NanoEngineering, Chemical Engineering Program, and Moores Cancer Center, University of California San Diego, La Jolla, CA 92093, USA.
*Corresponding author. Email: rhfang@ucsd.edu (R.H.F.); zhang@ucsd.edu (L.Z.)

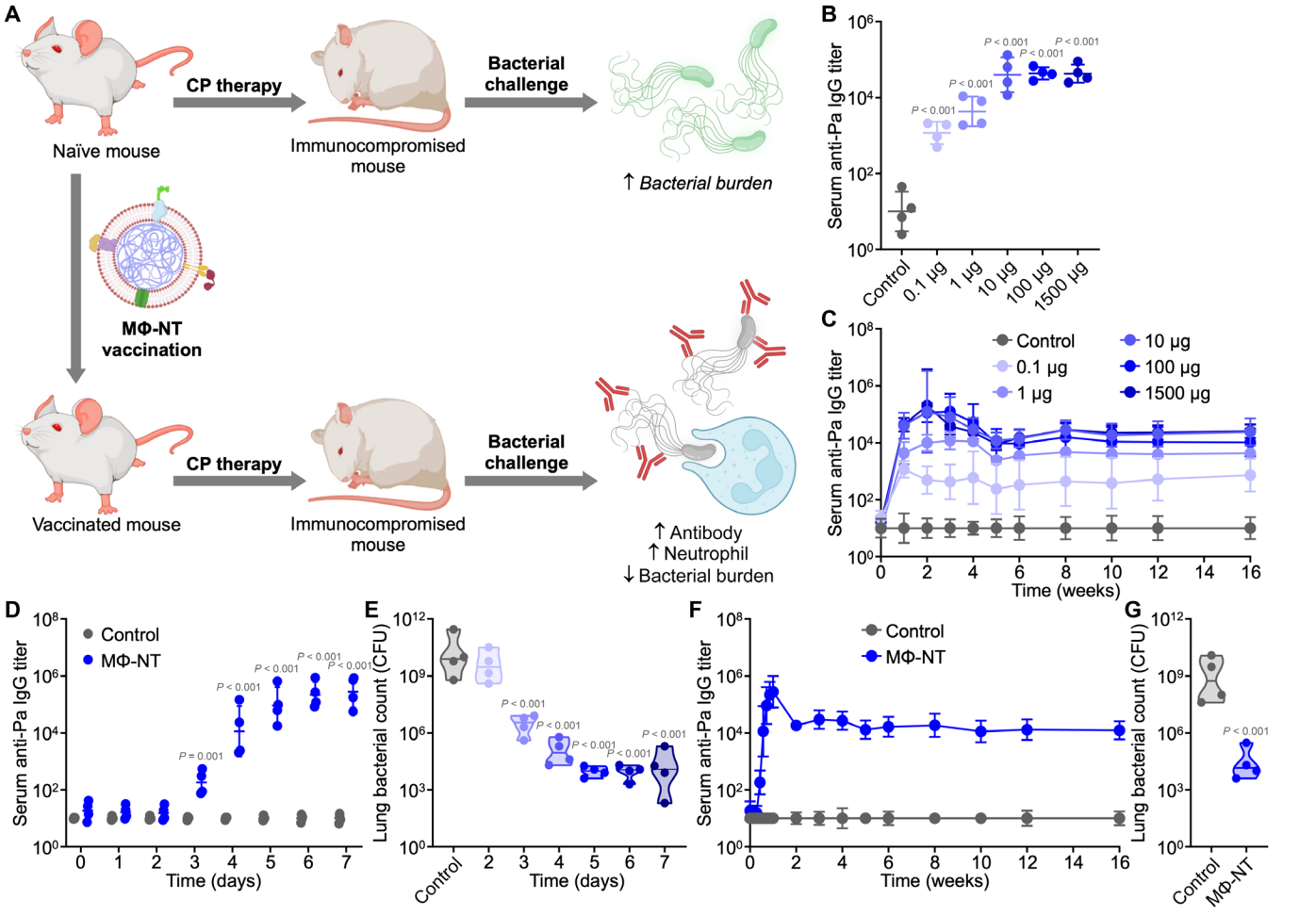

Fig. 1. Vaccination with MΦ-NT confers rapid and long-lasting immunity against *P. aeruginosa*. (**A**) Animals with CP-induced immunodeficiency are more susceptible to bacterial infection. In contrast, immunocompromised animals that have been previously vaccinated with MΦ-NT can effectively repel opportunistic infections through a combination of pathogen-specific antibodies and elevated neutrophils; created with BioRender. (**B**) Serum anti–*P. aeruginosa* (anti-Pa) IgG 7 days after vaccination with increasing amounts of MΦ-NT ($n = 4$, geometric mean ± SD). (**C**) Serum anti–*P. aeruginosa* IgG over time after vaccination with increasing amounts of MΦ-NT on days 0, 7, and 14 ($n = 4$, geometric mean ± SD). (**D**) Serum anti–*P. aeruginosa* IgG over 1 week after vaccination with 100 µg of MΦ-NT on day 0 ($n = 4$, geometric mean ± SD). (**E**) Lung bacterial load of mice intratracheally challenged with 10^7 CFU *P. aeruginosa* at increasing times after vaccination with 100 µg of MΦ-NT ($n = 4$, geometric median). (**F**) Serum anti–*P. aeruginosa* IgG over time after vaccination with 100 µg of MΦ-NT on day 0 ($n = 4$, geometric mean ± SD). (**G**) Lung bacterial load of mice intratracheally challenged with 10^7 CFU *P. aeruginosa* 4 months after vaccination with 100 µg of MΦ-NT ($n = 4$, geometric median).

fabricated with plasma membrane sourced from human cell lines, highlighting the clinical potential of this vaccination strategy.

RESULTS

MΦ-NT elicits rapid, long-lasting immunity

MΦ-NT was synthesized by using macrophage membrane-coated nanoparticles (MΦ-NPs) to neutralize protein fractions isolated from cultures of the *P. aeruginosa* P4 clinical isolate, which secretes both hemolytic and cytotoxic virulence factors (*24*, *36*). It is important to note that, in their native form, these bacterial protein secretions cannot be safely administered in vivo due to considerable toxicity concerns (*24*). We confirmed that, after being formulated into MΦ-NT, the hemolytic activity of isolated *P. aeruginosa* secretions (PaS) was completely attenuated (fig. S1). Previously, proteomic analysis has been used to identify the PaS proteins that are preferentially bound to the nanoparticles (*24*). Subcutaneous injection of MΦ-NT did not significantly affect body weight, and there were negligible effects on the number of circulating blood cells and serum biomarker levels (fig. S2). To evaluate the dose-response relationship, increasing amounts of MΦ-NT were subcutaneously administered into mice, and circulating immunoglobulin G (IgG) antibodies in the serum were analyzed. High levels of antibodies specific for *P. aeruginosa* were detected 1 week after the vaccination (Fig. 1B). At this time point, the antibody titers were saturated with 10 µg of MΦ-NT, and further increases in dosage did not significantly alter the immune response. The immune response appeared to have saturated after only 7 days, as boosters administered at 1 and 2 weeks after the initial vaccination did not further increase antibody titer levels (Fig. 1C and fig. S3). The antibody response elicited by MΦ-NT stabilized after a month and remained elevated for at least 4 months. A MΦ-NT dosage of 100 µg was used for all subsequent studies to ensure antibody titer saturation.

To further dissect the short-term kinetics of the immune response to MΦ-NT, titers were monitored daily for a week after a single-dose immunization (Fig. 1D). Antibody levels began to rise 3 days after injection and peaked after approximately 5 days. As *P. aeruginosa* is one of the leading causes of lung infections (*6*, *37*), we examined whether the rapidly produced antibodies conferred protection in a pneumonia model. Animals were intratracheally challenged with *P. aeruginosa* at varying times after vaccination, and the bacterial burden in the lungs was quantified after 1 day (Fig. 1E). A strong inverse correlation between antibody titer levels and bacterial burden was observed. With increasing time between vaccination and bacterial challenge, the bacterial count in the lungs progressively decreased until reaching a minimum at 5 days after vaccination. With just a single dose of MΦ-NT, anti-*P. aeruginosa* titer levels stabilized after 2 weeks and remained constant for a minimum of 4 months (Fig. 1F and fig. S4). The persistent serum antibodies were indicative of long-lasting immunity, as mice challenged 4 months after vaccination were capable of strongly resisting *P. aeruginosa* lung infections (Fig. 1G).

CP induces leukopenia and increases susceptibility to bacterial infection

To evaluate the clinical relevance of MΦ-NT in high-risk populations, a chemotherapy-induced animal model of immunodeficiency was used. CP is clinically used to treat cancer, autoimmune diseases, and transplant rejections, and the drug has been widely used to investigate the potential effectiveness of various medical interventions in immunocompromised individuals (*38*–*40*). Following the intraperitoneal injection of CP at a dosage of 150 mg kg^{-1} into mice, the effects on major white blood cell (WBC) populations in the peripheral blood were monitored daily (Fig. 2, A to F, and fig. S5). One day after CP treatment, there was a drop in circulating T cells, B cells, dendritic cells, macrophages, inflammatory monocytes, and neutrophils. Most notably, the number of B cells declined by more than 20-fold, while macrophages and inflammatory monocytes were reduced by roughly 10-fold. Immune cell counts remained low for several days, with some signs of recovery for myeloid lineage cells after 4 days.

A major reduction in disease-fighting immune cell subsets can lead to a compromised immune system and an increased risk to bacterial infections. To confirm this effect, leukodepleted and healthy mice were intratracheally infected with increasing numbers of *P. aeruginosa* (Fig. 2G). It was evident that mice with CP-induced immunodeficiency were more susceptible to infection, with higher mortality rates compared to healthy mice. Accordingly, bacterial burden in the lungs was also significantly higher for CP-treated mice than for healthy mice at the same challenge dose (Fig. 2H). In addition to pneumonia, *P. aeruginosa* commonly infects the bloodstream and can cause life-threatening sepsis (*7*). Similar trends were observed in a septicemia infection model, where leukodepleted mice more readily succumbed to *P. aeruginosa* challenge (Fig. 2I). CP-treated mice also had consistently higher bacterial burdens in all major organs that were examined compared to healthy mice (Fig. 2J).

Subcutaneous vaccination with MΦ-NT protects immunodeficient mice against infection

After confirming that CP treatment could increase susceptibility to bacterial infection, the benefits of MΦ-NT vaccination were next investigated in immunodeficient mice. Animals were subcutaneously

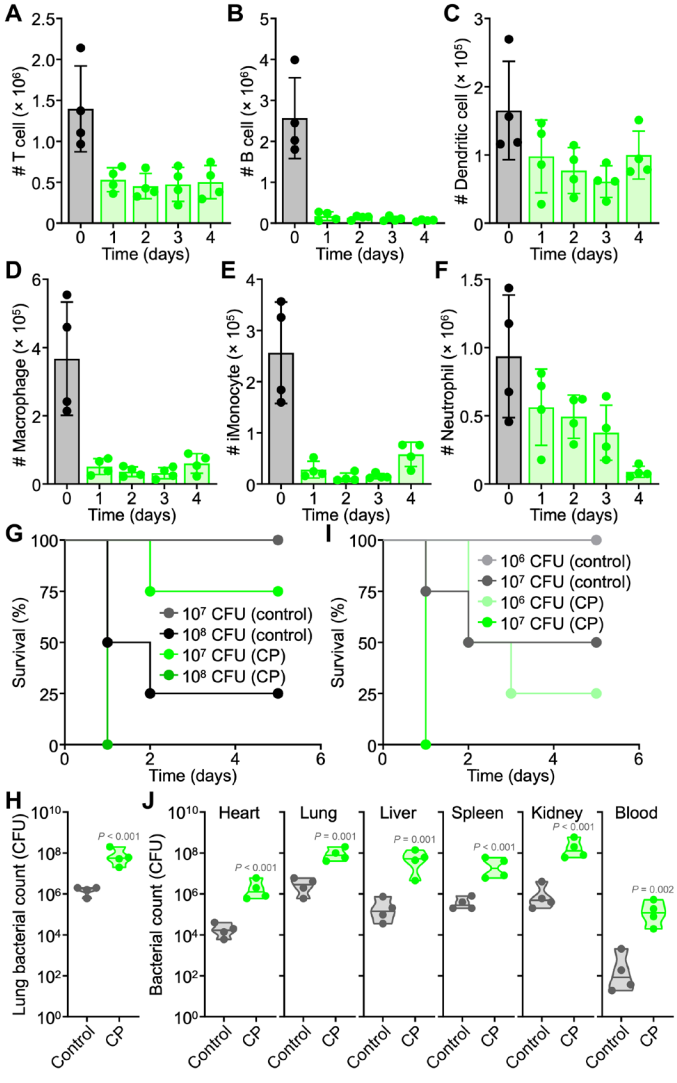

Fig. 2. CP treatment depletes immune cells and increases susceptibility to bacterial infection. (**A** to **F**) Number of T cells (A), B cells (B), dendritic cells (C), macrophages (D), inflammatory monocytes (E), and neutrophils (F) per 1 ml of blood on increasing days after CP treatment ($n = 4$, mean ± SD). (**G**) Survival of naïve and CP-treated mice intratracheally challenged with increasing numbers of *P. aeruginosa* ($n = 4$). (**H**) Lung bacterial load of naïve and CP-treated mice intratracheally challenged with 10^7 CFU *P. aeruginosa* ($n = 4$, geometric median). (**I**) Survival of naïve and CP-treated mice intravenously challenged with increasing numbers of *P. aeruginosa* ($n = 4$). (**J**) Bacterial load in naïve and CP-treated mice intravenously challenged with 10^6 CFU *P. aeruginosa* ($n = 4$, geometric median).

administered with MΦ-NT in the neck region on day 0, intraperitoneally treated with CP on day 5, and then challenged with *P. aeruginosa* on day 7. Immediately before infection, serum samples were collected to assess for anti–*P. aeruginosa* titers (Fig. 3A). MΦ-NT vaccination induced strong antibodies that were four orders of magnitude higher than for unvaccinated control mice. The basal titer levels in CP-treated mice dropped subtly compared with healthy controls, potentially due to the drastic depletion of circulating B cells (*41*). In contrast, CP-treated mice that were previously vaccinated with MΦ-NT had antibody titers that were comparable to those of immunocompetent animals that were also vaccinated.

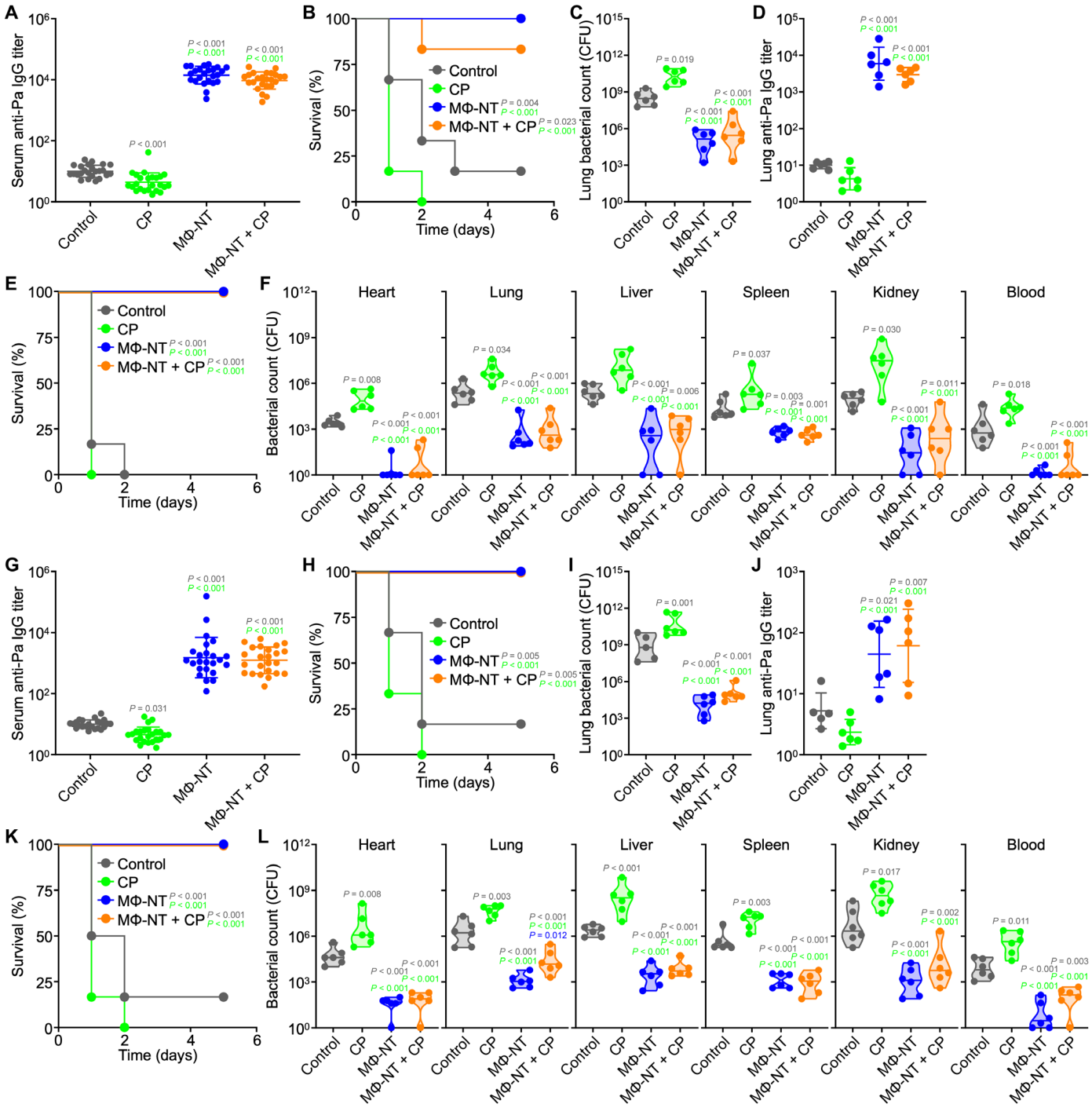

Fig. 3. Vaccination with MΦ-NT protects immunocompromised animals from *P. aeruginosa* pneumonia and septicemia. Mice were subcutaneously (**A** to **F**) or intranasally (**G** to **L**) vaccinated on day 0, administered CP on day 5, and challenged with *P. aeruginosa* on day 7. (A) Serum anti–*P. aeruginosa* IgG preceding infection ($N = 24$ pooled from four independent experiments, geometric mean ± SD). (B) Survival of mice intratracheally challenged with 10^8 CFU ($n = 6$). (C and D) Lung bacterial load (C) and anti-*P. aeruginosa* IgG (D) 1 day after intratracheal challenge with 10^7 CFU [$n = 6$, geometric median (C) and geometric mean ± SD (D)]. (E) Survival of mice intravenously challenged with 10^7 CFU ($n = 6$). (F) Bacterial load in mice 1 day after intravenous challenge with 10^6 CFU ($n = 6$, geometric median). (G) Serum anti–*P. aeruginosa* IgG preceding infection ($N = 24$ pooled from four independent experiments, geometric mean ± SD). (H) Survival of mice intratracheally challenged with 10^8 CFU ($n = 6$). (I and J) Lung bacterial load (I) and anti–*P. aeruginosa* IgG (J) 1 day after intratracheal challenge with 10^7 CFU [$n = 6$, geometric median (I) and geometric mean ± SD (J)]. (K) Survival of mice intravenously challenged with 10^7 CFU ($n = 6$). (L) Bacterial load in mice 1 day after intravenous challenge with 10^6 CFU ($n = 6$, geometric median).

The protective efficacy was first evaluated in a *P. aeruginosa* pneumonia model (Fig. 3B). Vaccinated mice that did not receive CP treatment all survived the bacterial infection, whereas most of the unvaccinated CP-treated and naïve mice succumbed within 3 days. Encouragingly, protection was evident in CP-treated mice that were previously vaccinated with MΦ-NT, with five of six animals surviving the challenge. The results correlated well with those from a subsequent enumeration study, where the bacterial burdens in the lungs of all vaccinated mice, regardless of immune status, were significantly lower than those of the unvaccinated CP-treated and naïve mice (Fig. 3C). When analyzing the titers in lung homogenates post infection, high levels of *P. aeruginosa*–specific IgGs were detected in samples from vaccinated mice, suggesting that the protective effects were mediated at least in part by the presence of these antibodies (Fig. 3D).

Protection against infection was additionally examined using a septicemia model (Fig. 3E). In this case, all mice immunized with MΦ-NT survived a lethal intravenous challenge with *P. aeruginosa*. On the contrary, all unvaccinated mice in the CP-treated and naïve groups succumbed quickly to the infection. In a follow-up enumeration study, the bacterial burden in major organs such as the heart, lungs, liver, spleen, and kidneys after systemic challenge with *P. aeruginosa* was significantly lower for immunized mice (Fig. 3F). In contrast, the bacterial load in unvaccinated CP-treated mice was significantly elevated compared with unvaccinated control mice. Overall, these results provided encouraging evidence that MΦ-NT vaccination can act as a safeguard against the increased risks of infection associated with acquired immunodeficiency, offering protection similar to what could be achieved in fully immunocompetent individuals.

Intranasal vaccination with MΦ-NT protects immunodeficient mice against infection

While subcutaneous administration is commonly used in preclinical studies, it is not ideal in a clinical setting due to the need for properly trained medical professionals. Furthermore, the painful jab of a needle can discourage a subset of patients, particularly those with trypanophobia, from receiving the vaccine (*42*). To circumvent this obstacle, the feasibility and effectiveness of MΦ-NT vaccination via the intranasal route was evaluated. Intranasal vaccination was effective at eliciting high serum IgG antibody titers against *P. aeruginosa*, albeit at a lower magnitude compared with subcutaneous vaccination (Fig. 3G). Despite the lower antibody levels, immunodeficient mice intranasally vaccinated with MΦ-NT were fully protected from an otherwise lethal lung infection (Fig. 3H), and this correlated with a low bacterial load in the lungs (Fig. 3I). Anti–*P. aeruginosa* titers in the lungs of intranasally vaccinated animals after infection were significantly higher than for unvaccinated mice, but the difference was smaller compared to what we observed when using subcutaneous vaccination (Fig. 3J). As before, strong efficacy was observed in a septicemia model of *P. aeruginosa* infection (Fig. 3, K and L). The lower number of antibodies produced via intranasal vaccination was likely due to the various mucosal barriers hindering the effective delivery of MΦ-NT to immune cells (*43*), although this may be readily overcome with further dose and schedule optimizations.

Passive transfer of immune sera reduces bacterial burden

Encouraged by the fact that MΦ-NT was efficacious in counteracting the increased susceptibility to *P. aeruginosa* infection associated with immunodeficiency, the protection mechanism was explored in-depth. The strong correlation between high antibody titers and improved health outcomes in the pneumonia and septicemia models indicated that humoral immunity was likely to have played a major role. To confirm this hypothesis, the serum from mice vaccinated with MΦ-NT was intravenously administered into naïve animals followed by *P. aeruginosa* challenge. In a pneumonia model, this passive vaccination using immune sera provided recipient mice with significant protection from bacterial infection (Fig. 4A). The protection was comparable to what was observed for mice actively vaccinated with MΦ-NT. Similar results were observed in a septicemia model (Fig. 4B). The studies were repeated in a therapeutic setting, where naïve mice were initially infected with bacteria before treatment with immune sera (Fig. 4, C and D). Although the reduction in bacterial burden was not as robust when comparing to the prophylactic setting, mice receiving the passive vaccination were still better protected from infection when compared to animals receiving control sera from naïve donors.

Neutrophils mediate the clearance of *P. aeruginosa* from vaccinated immunodeficient mice

While antibodies can recognize and opsonize pathogens, these proteins alone cannot eradicate bacteria. To identify the specific cell types involved in immune clearance, the lungs of intratracheally infected mice were collected for immunophenotyping (Fig. 4, E and F, and fig. S6). Compared to uninfected mice, infection led to a significant increase of dendritic cells and neutrophils in the lungs. Vaccination with MΦ-NT did not appear to alter the magnitude of immune cell increase. Animals pretreated with CP experienced a near-complete abrogation in innate immune cell recruitment, whereas there was a recovery of the dendritic cell and neutrophil responses in immunodeficient mice that previously received the MΦ-NT vaccine. When analyzing the peripheral blood in a septicemia model, a similar trend of increased circulating dendritic cells and neutrophils in immunodeficient mice receiving the MΦ-NT vaccine was noted (Fig. 4, G and H, and fig. S7). An interesting observation here was that naïve-infected mice had lower numbers of circulating T cells, B cells, macrophages, and inflammatory monocytes compared to uninfected mice, a drop that may be attributed to the fact that *P. aeruginosa* infection is known to induce lymphocyte apoptosis (*44*) and impair innate immune cells (*45*, *46*). Mice vaccinated with MΦ-NT, however, did not exhibit a decline in leukocyte counts. Analysis of the spleen after infection in the septicemia model also revealed an elevation in neutrophil counts, although the recovery in response for immunodeficient mice receiving MΦ-NT was not as profound (fig. S8). Together, the trends from these data showed the importance of neutrophil recruitment in the response against *P. aeruginosa* infection (*30*, *47*, *48*).

Neutrophil transfusion therapy rescues mice with severe leukopenia

The protective capacity of MΦ-NT was assessed in a more aggressive immunodeficiency model. Mice were pretreated with three doses of CP every other day starting 5 days after vaccination, followed by *P. aeruginosa* challenge 1 day after the last injection. Leukodepletion was severe, with nearly undetectable levels of all WBC populations in the peripheral blood (fig. S9). While mice receiving MΦ-NT exhibited high anti–*P. aeruginosa* titers (Fig. 4I), the vaccination did not effectively protect against infection, and a high bacterial burden was observed (Fig. 4J and fig. S10A). Regardless, there were some

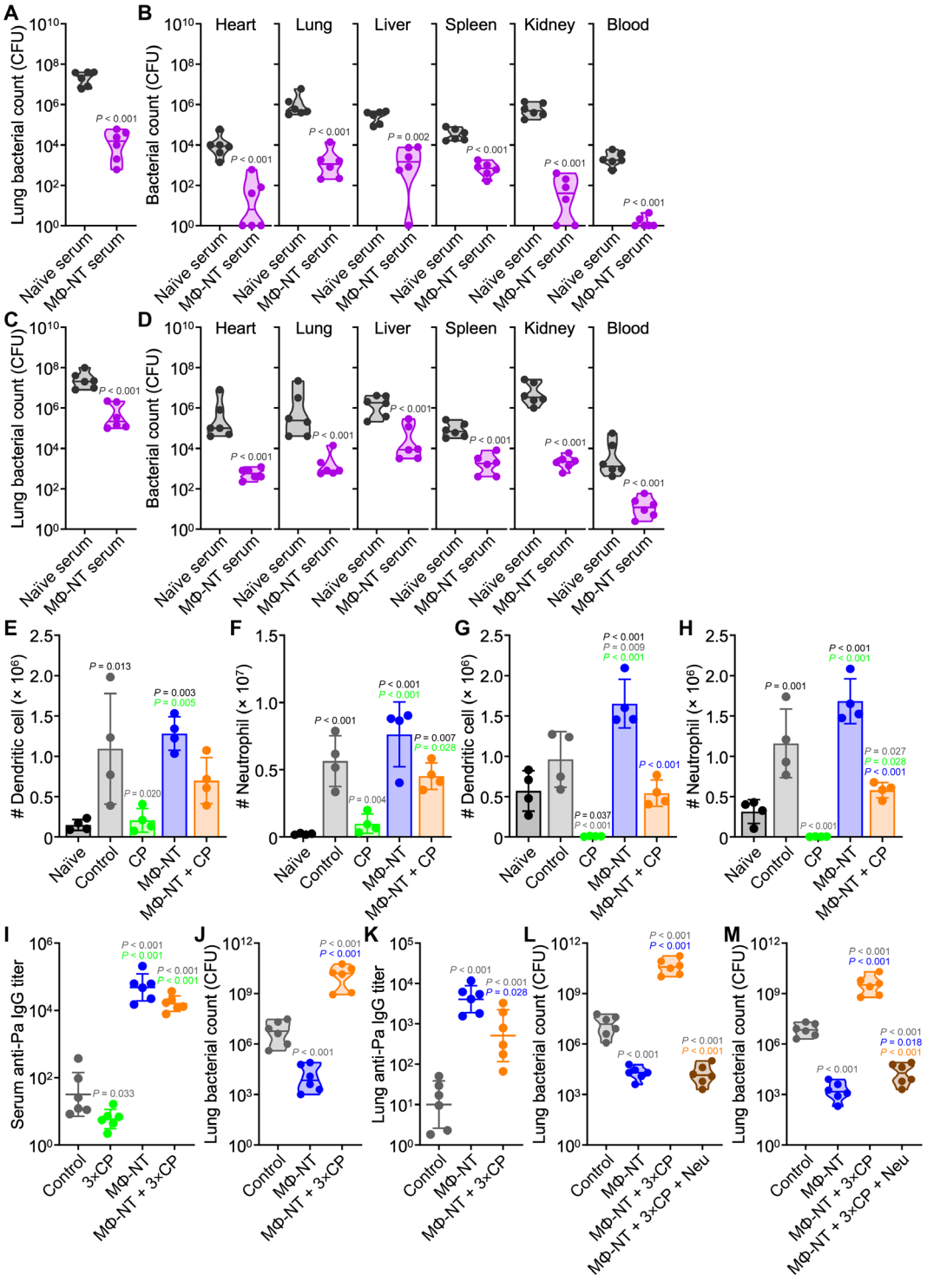

Fig. 4. MΦ-NT protection is mediated by antibodies and neutrophils. (**A** and **B**) Bacterial load in mice prophylactically immunized with sera and intratracheally (A) or intravenously (B) challenged with 10^7 or 10^6 CFU *P. aeruginosa*, respectively ($n = 6$, geometric median). (**C** and **D**) Bacterial load in mice intratracheally (C) or intravenously (D) challenged with 10^7 or 10^6 CFU *P. aeruginosa*, respectively, and therapeutically treated with sera ($n = 6$, geometric median). In (**E**) to (**H**), mice were subcutaneously vaccinated on day 0, administered CP on day 5, and challenged with *P. aeruginosa* on day 7. (**E** and **F**) Dendritic cells (E) and neutrophils (F) per lung 1 day after intratracheal challenge with 10^7 CFU ($n = 4$, mean ± SD). (**G** and **H**) Dendritic cells (G) and neutrophils (H) per 1 ml of blood 1 day after intravenous challenge with 10^6 CFU ($n = 4$, mean ± SD). In (**I**) to (**M**), mice were subcutaneously vaccinated on day 0; administered CP on days 5, 7, and 9; and intratracheally challenged with 10^6 CFU of *P. aeruginosa* on day 10. (I) Serum anti–*P. aeruginosa* IgG preceding infection ($n = 6$, geometric mean ± SD). (J) Lung bacterial load 1 day after challenge ($n = 6$, geometric median). (K) Lung anti–*P. aeruginosa* IgG 1 day after challenge ($n = 6$, geometric mean ± SD). (L and M) Lung bacterial load of mice prophylactically (L) or therapeutically (M) infused with 2×10^6 neutrophils (Neu) ($n = 6$, geometric median).

encouraging signs of efficacy as a major portion of the severely immunodeficient mice that did not receive the nanovaccine succumbed to infection before the experimental endpoint. Among the two surviving mice, their bacterial burden was significantly higher than for the immunodeficient mice immunized with MΦ-NT. After infection, antibody levels in the lungs of all vaccinated mice were elevated but significantly lower in the immunodeficient animals compared with their immunocompetent counterparts (Fig. 4K and fig. S10B).

While it was shown that MΦ-NT vaccination could lower *P. aeruginosa* numbers in severely immunocompromised hosts, the bacterial burden remained unacceptably high. Given our observations that neutrophils were the most significantly elevated compared with other immune cell types during the response to *P. aeruginosa* infection, we sought to determine whether neutrophil transfusion could work in conjunction with MΦ-NT vaccination to lower bacterial burden in the case of severe immunodeficiency. Granulocyte infusion therapy is commonly used in the clinic to treat bacterial infections in neutropenic patients, and the side effects of GVHD are markedly lower for those who are severely immunocompromised (*49*). Animals were vaccinated with MΦ-NT and subjected to aggressive leukodepletion by multiple CP treatments. Two hours before bacterial challenge, a group of mice was infused with primary neutrophils derived from healthy donors (Fig. 4L). In a pneumonia model, this prophylactic neutrophil transfusion protected immunocompromised hosts that received MΦ-NT from the infection, with efficacy equivalent to what was observed for healthy vaccinated mice. The treatment effect was further evaluated in a more clinically relevant therapeutic setting, where the neutrophil transfusions were performed after infection (Fig. 4M). Again, significant efficacy was observed, with neutrophil transfusion lowering the bacterial burden of vaccinated mice with severe immunodeficiency to levels near that of vaccinated immunocompetent mice. While supplementing neutrophils in the absence of vaccination would likely also have an antibacterial effect, the results from our passive immunization study suggested that maximal efficacy requires *P. aeruginosa*-specific titers, such as those elicited by MΦ-NT. Together, the data indicated that the immunity conferred by MΦ-NT vaccination is mediated by a combination of anti–*P. aeruginosa* antibodies and neutrophils, likely via a mechanism of opsonic phagocytosis (*50*); in vaccinated individuals with severe leukopenia, immunity can be restored by neutrophil transfusion therapy.

Vaccination with MΦ-NT protects aged mice against infection

In addition to hospital patients, another population that is at high risk of acquiring serious infections is the elderly, as immune function can decrease dramatically with age. We therefore investigated the ability of MΦ-NT to protect against *P. aeruginosa* infection in mice that were aged to 72 weeks (*51*). The aged mice had noticeably lower numbers of circulating T cells and B cells, while the number of dendritic cells, macrophages, and neutrophils were elevated (Fig. 5, A to F). Before vaccination, it was observed that the aged mice had significantly higher basal levels of antibodies against *P. aeruginosa*

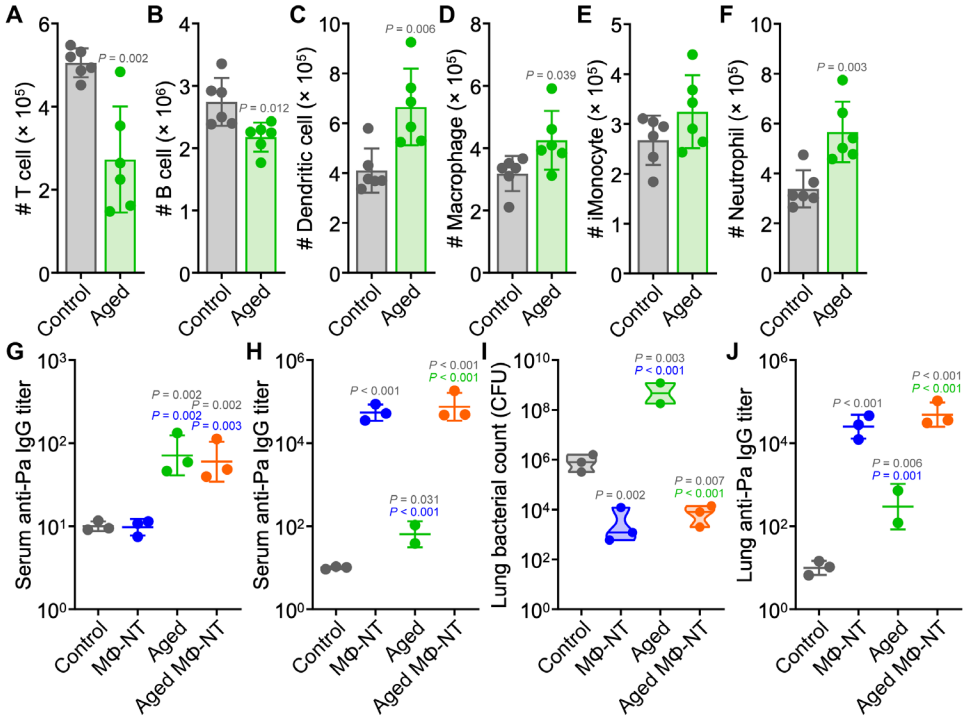

Fig. 5. Protective efficacy of MΦ-NT in aged mice. (**A** to **F**) Number of T cells (A), B cells (B), dendritic cells (C), macrophages (D), inflammatory monocytes (E), and neutrophils (F) per 1 ml of blood in 72-week-old mice ($n = 6$, mean ± SD). In (**G**) and (**H**), mice were subcutaneously vaccinated on day 0 and intratracheally challenged with 10^6 CFU *P. aeruginosa* on day 7. (G) Serum anti–*P. aeruginosa* IgG before vaccination ($n = 3$, geometric mean ± SD). (H) Serum anti–*P. aeruginosa* IgG preceding infection ($n = 2$ for "aged" group and $n = 3$ for all other groups, geometric mean ± SD). (**I** and **J**) Lung bacterial load (I) and anti–*P. aeruginosa* IgG (J) 1 day after challenge [$n = 2$ for "aged" group and $n = 3$ for all other groups, geometric median (I) and geometric mean ± SD (J)].

(Fig. 5G). After MΦ-NT vaccination, anti–*P. aeruginosa* titers were elevated to similar levels in both young and aged animals (Fig. 5H). One naïve aged mouse exhibited signs of morbidity unrelated to the experiment and was euthanized before bacterial challenge. Following intratracheal challenge with *P. aeruginosa*, all vaccinated mice had similar bacterial burden and antibody levels in their lungs (Fig. 5, I and J). On the other hand, aged mice that did not receive the MΦ-NT vaccine were more susceptible to infection and succumbed before the experimental endpoint. Postmortem enumeration revealed significantly higher bacterial burden in the lungs of these mice compared with young unvaccinated mice.

MΦ-NT fabricated with human cell membrane are effective against *P. aeruginosa*

For clinical application, MΦ-NT manufacturing should ideally use plasma membrane of human origins to minimize undesirable cross-species immune reactions. As the immune system is constantly exposed to self-antigens, the chance of a species-matched cell membrane coating inducing autoimmunity is low (*52*, *53*). The feasibility of generating a human MΦ-NT (hMΦ-NT) formulation was assessed by substituting the original murine plasma membrane with membrane from THP-1 cells during the nanoparticle coating process (*54*). Consistent with previous reports, the nanoparticles were larger after membrane coating, and their size further increased to roughly 125 nm after complexation with *P. aeruginosa* antigens (Fig. 6A). The zeta potential of the nanoparticles decreased upon coating (Fig. 6B), and transmission electron microscopy (TEM) images revealed a solid core wrapped by a thin shell of membrane (Fig. 6C). In terms of size, the hMΦ-NT was stable in solution at 4°C for at least 4 weeks (Fig. 6D). It has previously been established that cell membrane–coated nanoformulations can be lyophilized for long-term storage (*55*).

The successful neutralization of *P. aeruginosa* virulence factors on the final hMΦ-NT formulation was verified in a set of safety experiments. When incubated with red blood cells (RBCs), virulence factors from PaS induced significant hemolysis, but the hemolytic activity was completely neutralized in hMΦ-NT (Fig. 6E). Likewise, PaS caused significant cytotoxicity in murine macrophages, and this toxicity was likewise abrogated in hMΦ-NT (Fig. 6F). These results further highlighted the role of biomimetic cell membrane-coated nanoparticles in negating the toxicity of bacterial virulence factors. After confirming safety, the efficacy of hMΦ-NT as a vaccine was assessed by administering the formulation subcutaneously into mice. Similar to when using murine MΦ-NT, hMΦ-NT vaccination elicited strong antibody titers specific for *P. aeruginosa* and lowered bacterial burden in the lungs of immunodeficient mice (Fig. 6, G to I), suggesting that the immunogenicity of the formulation was driven largely by the PaS content and not any species-specific characteristic of the cellular membrane. Ultimately, MΦ-NT is a potent vaccine platform that can be utilized to protect highly susceptible immunocompromised populations from opportunistic infections by promoting remarkably specific and rapid immunity.

DISCUSSION

In summary, we have demonstrated the effectiveness of a nanotoxoid vaccine in safeguarding immunodeficient populations from opportunistic bacterial infections. The nanovaccine rapidly triggered robust antibacterial immunity that persisted for at least 4 months. In pneumonia and septicemia models of infection, vaccinated animals were strongly protected regardless of their immune status. Immunity was mediated primarily by the presence of highly specific antibodies along with the recruitment of neutrophils. As the antibodies elicited by nanotoxoids were largely unaffected by subsequently acquired immunodeficiency, our data suggest that even highly vulnerable patients who become severely leukopenic after vaccination can be rescued from otherwise fatal infections when receiving supplemental neutrophil transfusion therapy. While the

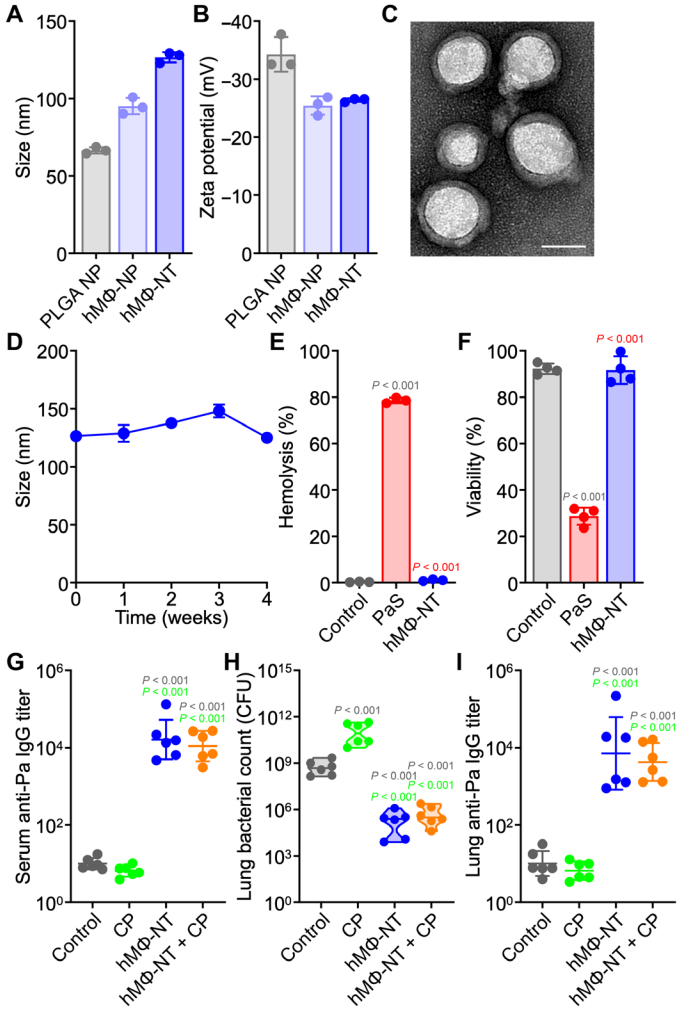

Fig. 6. MΦ-NT can be fabricated using human cell membrane. (**A** and **B**) Size (A) and zeta potential (B) of bare PLGA nanoparticle (NP), human MΦ-NP (hMΦ-NP), and hMΦ-NT ($n = 3$, mean ± SD). (**C**) Representative TEM image of hMΦ-NT. Scale bar, 50 nm. (**D**) Stability of hMΦ-NT over time ($n = 3$, mean ± SD). (**E**) Hemolysis of RBCs after incubation with control 10% sucrose, a PaS mixture, and hMΦ-NT at 37°C for 30 min ($n = 3$, mean ± SD). (**F**) Cell viability of J774A.1 cells after incubation with control 10% sucrose, a PaS mixture, and hMΦ-NT at 37°C for 3 days ($n = 4$, mean ± SD). In (G) to (I), mice were subcutaneously vaccinated with hMΦ-NT on day 0, administered CP on day 5, and intratracheally challenged with 10^7 CFU *P. aeruginosa* on day 7. (**G**) Serum anti–*P. aeruginosa* IgG preceding infection ($n = 6$, geometric mean ± SD). (**H**) Lung bacterial load 1 day after challenge ($n = 6$, geometric median). (**I**) Lung anti–*P. aeruginosa* IgG 1 day after challenge ($n = 6$, geometric mean ± SD).

bulk of our studies were performed using nanotoxoids manufactured with murine cell membrane, similar protection against infection was observed when a human membrane source was used. With their ease of synthesis, excellent safety profile, and favorable storage conditions, nanotoxoid vaccines have immense clinical translation potential. To produce nanotoxoids in clinically relevant quantities, focus will need to be placed on reducing batch-to-batch variability, developing assays to support quality control, and adapting established industrial-scale processes for protein production and nanoparticle synthesis. Since effective immunity can be realized using accessible routes of administration, we envision patients can be easily vaccinated before undergoing procedures or therapies that may lead to immunodeficiency. While the current study was focused on *P. aeruginosa*, the approach may be readily applied to other highly virulent antibiotic-resistant superbugs for which effective vaccines have remained elusive. In the future, more detailed immunological characterization can be performed to better understand the contributions of various memory cell populations and the role of adaptive cellular immunity. Ultimately, continued development on nanotoxoid vaccines, with their inherently multiantigenic nature and ease of customization, could contribute considerably to the clinical management of nosocomial infections.

MATERIALS AND METHODS

Cell lines and culture

J774A.1 (TIB-67), a murine macrophage cell line isolated from female BALB/c mice, and THP-1 (TIB-202), a human monocyte cell line derived from an acute monocytic leukemia patient, were purchased from the American Type Culture Collection and cultured at 37°C with a humidified atmosphere of 5% CO_2 in T175 suspension flasks (Genesee Scientific) using Dulbecco's modified Eagle's medium (Corning) or Roswell Park Memorial Institute 1640 medium (Gibco) supplemented with 10% (v/v) bovine growth serum (Hyclone) and 1% (v/v) penicillin-streptomycin (Gibco). To harvest the cells, the media were collected, and any adherent cells were detached with 5 mM EDTA in phosphate-buffered saline (PBS; Corning). Cells were spun down at 700*g* for 5 min, resuspended in a 1:1 mixture of complete medium and cryopreservation medium (Hyclone), and stored at −80°C. Plasma membrane was derived as previously reported (*56*, *57*). All cell lines were tested for mycoplasma contamination monthly with a polymerase chain reaction detection kit (Applied Biological Materials).

P. aeruginosa culture and toxin purification

The multidrug-resistant *P. aeruginosa* P4 clinical isolate was a gift from the V. Nizet laboratory and stored at −80°C (*36*). The bacterial stock was first streaked onto LB (Becton Dickinson) agar plates. After overnight incubation at 37°C, a single colony was cultured in a rotatory shaker at 200 rpm with 5 ml of liquid LB media. One day later, the culture was diluted 1:100 into fresh medium, and the *P. aeruginosa* were spun down at 4500*g* for 20 min after another day of incubation. The resulting protein-rich supernatant was filtered through a 0.22-μm polyethersulfone vacuum filter (Millipore Sigma) and stored at −80°C. For infections, refreshed *P. aeruginosa* was cultured between 4 and 6 hours until exponential growth and pelleted at 4500*g* for 20 min at 4°C. The bacteria were washed once with PBS and then resuspended in PBS at the appropriate concentrations for inoculation. The bacteria colony-forming unit (CFU) concentration was estimated by measuring the optical density of the solution at 600 nm.

To collect the secreted virulence factors, 90 ml of saturated ammonia sulfate (Thermo Fisher Scientific) solution was added dropwise into 30 ml of *P. aeruginosa* supernatant while stirring on ice. After 1 hour, protein precipitates were spun down at 5000*g* for 20 min, and the pellet was resuspended in deoxyribonuclease (DNase)/ribonuclease (RNase)–free distilled water (Invitrogen). The supernatant was collected, and 13.55 g of solid ammonia sulfate was slowly added for a second precipitation. After stirring overnight, precipitated proteins were pelleted, resuspended, and combined with the sample from the first round of precipitation. The pooled protein suspension was desalted by size-exclusion chromatography with a fine G-25 Sephadex column (Millipore Sigma). Two protein-rich peaks were observed by measuring the absorbance at 280 nm with a TECAN Spark 20M multimode microplate reader, and the protein-containing fractions corresponding to these peaks were consolidated and then concentrated using Amicon centrifugal filters with a 3-kDa nominal molecular weight limit (NMWL) (Millipore Sigma). The consolidated fractions from the first and second protein peaks were designated PaS-1 and PaS-2, respectively (*24*). The toxin purification process was repeated several times, and all PaS-1 or PaS-2 collections were pooled together to minimize batch variation. The fractions were stored at 4°C until use, and protein content was determined with a Rapid Gold BCA protein assay kit (Pierce) according to the manufacturer's instructions.

MΦ-NT fabrication and characterization

Polymeric nanoparticles were synthesized by precipitating 1 ml of 0.66 dl g^{-1} carboxyl-terminated poly(lactic-*co*-glycolic acid) (PLGA; LACTEL Absorbable Polymers) dissolved at 10 mg ml^{-1} in acetone into 1 ml of 10 mM tris-HCl (pH 8.0; Corning). The acetone was evaporated under vacuum for at least 3 hours before macrophage membrane was mixed with the PLGA cores at a 1:1 membrane protein–to–polymer weight ratio. MΦ-NPs were then fabricated by sonicating the mixture in a Fisher FS30D bath sonicator for 2 min, after which 20 μg of PaS-1 and 0.5 μg of PaS-2 were mixed with 100 μg of MΦ-NP. The bacterial protein–to–nanoparticle ratio was optimized for safety to enable in vivo administration (*24*). Toxins were neutralized at 37°C for 15 min before the resulting MΦ-NT formulation was adjusted to 10% (w/v) sucrose (Millipore Sigma) and used without further purification. In the dose-response study, mice were subcutaneously vaccinated with varying amounts of MΦ-NT (0.1, 1, 10, 100, or 1500 μg; based on PLGA mass) in the neck region on day 0 followed by two booster doses on day 7 and day 14. For all other studies, animals either subcutaneously or intranasally received a single 100-μg dose of MΦ-NT.

To fabricate hMΦ-NT, the J774A.1 membrane was substituted with THP-1 membrane (*54*). The size and zeta potential of hMΦ-NT were measured by dynamic light scattering with a Malvern Zetasizer Lab Red Label. For TEM, samples were adsorbed onto a 400-mesh carbon film grid (Electron Microscopy Sciences) for 10 min and washed three times with water for 2 min each. The grid was then negatively stained with 1% (w/v) uranyl acetate (Electron Microscopy Sciences) for 15 s and visualized with a JEOL 1200 EX II electron microscope. For stability, hMΦ-NT was adjusted to 10% sucrose and kept at 4°C with regular size measurements.

To confirm successful toxin neutralization, 10% sucrose, 30 μg of PaS-1 and 0.75 μg of PaS-2, or 150 μg of hMΦ-NT was incubated

with 2.5% (v/v) RBCs purified from male CD-1 mice at 37°C for 30 min. Intact cells were spun down at 2000*g* for 5 min, and hemolysis was determined by analyzing the supernatant absorbance at 540 nm. Hemolysis for murine MΦ-NT was studied using the same experimental setup at different total PaS concentrations while maintaining the same PaS-1 to PaS-2 ratio. To determine cytotoxicity, J774A.1 were seeded into 96-well tissue culture plates (Genesee Scientific) at 6×10^3 cells per well and allowed to adhere overnight before the cells were incubated with 10% sucrose, 10 μg of PaS-1 and 0.25 μg of PaS-2, or 50 μg of hMΦ-NT for 3 days at 37°C. The medium was then removed, and the cells were washed with 200 μl of PBS before cell viability was determined using a CellTiter 96 AQueous One Solution cell proliferation assay (Promega) according to the manufacturer's instructions. Controls for 100% hemolysis and cytotoxicity were prepared by incubating the appropriate cells with 1% (v/v) Triton-X (Thermo Fisher Scientific).

Animal care

Male CD-1 mice (6 to 8 weeks) were purchased from Charles River Laboratories; female C57BL/6J mice (6 weeks) were purchased from the Jackson Laboratory and aged in-house to 72 weeks. Mice were housed in an animal facility at the University of California, San Diego (UCSD) under federal, state, local, and National Institutes of Health (NIH) guidelines. All animal experiments were performed in accordance with NIH guidelines and approved by the Institutional Animal Care and Use Committee of UCSD.

Biosafety studies

To confirm safety, 100 μg of MΦ-NT was subcutaneously injected into CD-1 mice near the neck region, and body weights were monitored daily for a week. At 1 day after vaccination, blood was collected via submandibular puncture into Microvette 100 potassium-EDTA blood collection tubes (Sarstedt) for cell quantification. To obtain serum samples for biochemistry analysis, blood was collected without an anticoagulant, allowed to coagulate for at least 30 min, and centrifuged at 3000*g* for 10 min. All tests were performed by the Animal Care Program Diagnostic Services Laboratory at UCSD.

Antibody titers

Anti–*P. aeruginosa* titer levels were determined by an enzyme-linked immunosorbent assay (ELISA). Pelleted *P. aeruginosa* were resuspended with DNase/RNase-free water and sonicated in a bath sonicator to induce lysis. The protein content of the lysed bacteria was determined using a Rapid Gold BCA assay, and the *P. aeruginosa* lysate was coated overnight at 4°C onto 96-well assay plates (Corning) at 1 μg per well in ELISA coating buffer (BioLegend). In the following day, the plates were blocked for 1 hour with 5% (w/v) milk (Apex Bioresearch Products) dissolved in PBS (Teknova) with 0.05% (v/v) Tween 20 (National Scientific) and then incubated with serially diluted samples for 2 hours followed by horseradish peroxidase–conjugated anti-mouse IgG (BioLegend) at a 1:2000 dilution for another 2 hours. The plates were developed with 3,3′,5,5′-tetramethylbenzidine substrate (BioLegend) for 10 min before the reaction was stopped with 1 N HCl (Thermo Fisher Scientific). The absorbance was read at 450 nm with 570 nm as the reference using a TECAN Spark 20M multimode microplate reader. All plates were washed at least four times with PBS containing 0.05% Tween 20 between each step, and incubation steps were performed at room temperature on a rotary shaker configured to 150 rpm.

Antibody titer levels were calculated by fitting the data to a four-parameter logistic curve, and the interpolation threshold was set such that the mean of the unmanipulated control mice was approximately 10^1. In the severe immunodeficiency model, the data were interpolated such that the average titers for the control groups were approximately $10^{1.5}$ due to the low signals for the 3×CP group. During the daily blood collections to obtain serum samples, care was taken to minimize the volume drawn to avoid the data being affected by significant blood loss. For lung samples, the tissues were first processed using a Biospec Mini-Beadbeater-16 in 1 ml of PBS with 2-mm zirconia beads (Biospec). The homogenates were then centrifuged at 10,000*g* for 10 min, and the supernatants were clarified through 0.22-μm polyvinylidene fluoride syringe filters (CellTreat). Samples were stored at −20°C if not used immediately.

Leukodepletion with CP

To evaluate WBC depletion after CP treatment, blood was collected daily from mice on days 0 through 4 by submandibular puncture using heparin (Millipore Sigma) as the anticoagulant. Immediately after the first collection, mice were intraperitoneally injected with CP (Millipore Sigma) at 150 mg kg^{-1}. In the severe immunodeficiency model, blood was sampled 1 day after the last of the CP injections, which were given on days 5, 7, and 9 after vaccine administration. For aged mice, blood was sampled 1 day before vaccination. RBCs were lysed with a commercial RBC lysis buffer (BioLegend) according to the manufacturer's instructions before the remaining cells were stained with a LIVE/DEAD fixable aqua dead cell stain kit (Life Technologies) for 30 min at room temperature. Cells were washed once with 1% (w/v) bovine serum albumin (BSA; Millipore Sigma) in PBS via centrifugation at 700*g* for 5 min, blocked with 1% BSA in PBS on ice for 15 min, and then incubated with TruStain FcX PLUS anti-mouse CD16/32 antibody (BioLegend) for 10 min. After the blocking steps, samples were stained with a cocktail containing Pacific Blue–conjugated anti-mouse CD19 (6D5), fluorescein isothiocyanate–conjugated anti-mouse CD3 (17A2), phycoerythrin (PE)–conjugated anti-mouse F4/80 (BM8), peridinin chlorophyll protein/cyanine5.5–conjugated anti-mouse Ly-6G (1A8), PE/cyanine7-conjugated anti-mouse Ly-6C (HK1.4), allophycocyanin (APC)–conjugated anti-mouse CD11c (N418), and APC/cyanine7-conjugated anti-mouse/human CD11b (M1/70) (all from BioLegend) for 30 min on ice and then washed with 1% BSA in PBS to remove the unbound antibodies. Last, the cells were resuspended in 1% BSA in PBS and mixed with CountBright absolute counting beads (Life Technologies). Data were acquired on a Becton Dickinson FACSCanto II flow cytometer and analyzed using FlowJo software. Single-stained and fluorescence-minus-one controls were prepared similarly for compensation and gating purposes. The cell concentration was calculated by comparing the ratio of cell events to counting bead events according to the manufacturer's instructions.

P. aeruginosa infection models

All mice were challenged with log-phase *P. aeruginosa* 2 days after CP treatment, except for the severe immunodeficiency model in which mice were challenged 1 day after the last CP injection. For the pneumonia model, mice were anesthetized with an intraperitoneal injection of ketamine (100 mg kg^{-1}; MWI Veterinary Supply) and xylazine (10 mg kg^{-1}; MWI Veterinary Supply). A 40-μl solution of the bacteria was then intratracheally inoculated with gel-loading pipette tips (Invitrogen) by allowing the mice to naturally breathe in the

liquid followed by 200 μl of air. In the septicemia model, 200 μl of *P. aeruginosa* was intravenously injected via the lateral tail vein. For studies involving the severe immunodeficiency model and aged mice, challenges were performed with 10^6 CFU of bacteria. Otherwise, bacterial dosages of 10^8 and 10^7 CFU were used for the pneumonia survival and enumeration experiments, respectively, whereas 10-fold lower dosages were employed for the corresponding septicemia studies. For the passive immunization studies, animals were intravenously inoculated with 200 μl of serum purified from either naïve or MΦ-NT vaccinated mice either 2 hours before or 1 hour after the infection.

To quantify bacterial load for the pneumonia model, mice were euthanized 1 day after challenge with *P. aeruginosa*, and their lungs were collected. For the septicemia model, blood was collected before euthanasia 1 day after challenge with *P. aeruginosa*, and the animals were perfused with at least 50 ml of PBS from the left ventricle through the right atrium before the heart, lungs, liver, spleen, and kidneys were collected. All organs were weighed and homogenized using a Biospec Mini-Beadbeater-16 in 1 ml of PBS with 2-mm zirconia beads. Samples were then serially diluted in PBS, and 50 μl of each dilution was plated onto LB agar plates. After overnight incubation at 37°C, the number of colonies was counted to calculate the bacterial load in each organ. For survival studies, mice were monitored daily for 5 days.

Immune response to *P. aeruginosa* infections

Mice were vaccinated with MΦ-NT on day 0, treated with CP on day 5, and challenged with *P. aeruginosa* on day 7 as before. For the pneumonia model, the lungs were collected 1 day after infection, cut into small 1- to 3-mm pieces, and digested at 37°C for 30 min in collagenase D (1 mg ml^{-1}; Roche) and DNase I (1 mg ml^{-1}; Roche) in Dulbecco's PBS with calcium and magnesium (Gibco). In the septicemia model, the spleen and blood were similarly collected 1 day after infection. The spleens were first physically sheared using a pipette. Dissociated lung and spleen tissues were then passed through a 70-μm mesh cell strainer (Thermo Fisher Scientific) to obtain single-cell suspensions, followed by treatment with RBC lysis buffer. All samples were analyzed by flow cytometry as previously described.

Neutrophil transfusion model

Mice were vaccinated with MΦ-NT on day 0 followed by CP treatment on days 5, 7, and 9. One day later, animals were intratracheally inoculated with 10^6 CFU of *P. aeruginosa*. Mice were intravenously infused with 2×10^6 primary neutrophils either 2 hours before or 1 hour after the challenge, and the bacterial burden in the lungs was quantified 1 day after bacterial challenge.

Neutrophils were derived following a previously published protocol (*58*). Briefly, CD-1 mice were first given an intraperitoneal injection of lipopolysaccharide (1.5 mg kg^{-1}) from *Escherichia coli* K12 (Invivogen). Six hours later, whole blood was collected via submandibular puncture using 10 mM EDTA as the anticoagulant and spun down at 3000*g* for 5 min. The supernatant was discarded, and the buffy coat was collected and carefully deposited onto a Percoll (Cytiva) gradient consisting of 78, 69, and 52% (v/v) layers, each 3 ml in volume. The sample was then centrifuged at 1500*g* for 30 min at 4°C with no brake, and neutrophils were collected from the 78% layer and the 78/69% interface. Last, the sample was diluted with PBS, spun down at 3000*g* for 5 min, and processed with RBC lysis buffer. To prepare the Percoll gradient, a 100% isotonic Percoll stock solution was initially prepared by mixing Percoll with DNase/RNase-free water and 20× PBS at an 18:1:1 ratio. Percoll solutions of varying concentrations were then obtained by diluting the 100% stock with PBS.

Data analysis

All data were analyzed with GraphPad Prism 8. Antibody titer levels are presented as the geometric mean ± SD, and bacterial burdens are visualized as violin plots with the geometric median. All other data are presented as the mean ± SD. A minimum sample size of $n = 3$ was used for all studies. Comparisons between two groups were performed using an unpaired two-tailed Student's *t* test, while one-way ANOVA followed by either Dunnett's multiple comparisons test (all groups compared with control only) or Tukey's post hoc analysis (all groups compared with each other) was used for comparison between more than two groups. The Mantel-Cox test was used to determine statistical significance between survival curves.

SUPPLEMENTARY MATERIALS

Supplementary material for this article is available at https://science.org/doi/10.1126/sciadv.abq5492

View/request a protocol for this paper from *Bio-protocol*.

REFERENCES AND NOTES

1. P. Dadgostar, Antimicrobial resistance: Implications and costs. *Infect. Drug Resist.* **12**, 3903–3910 (2019).
2. Antimicrobial Resistance Collaborators, Global burden of bacterial antimicrobial resistance in 2019: A systematic analysis. *Lancet* **399**, 629–655 (2022).
3. C. L. Ventola, The antibiotic resistance crisis: Part 1: Causes and threats. *Pharm. Ther.* **40**, 277–283 (2015).
4. H. Wisplinghoff, T. Bischoff, S. M. Tallent, H. Seifert, R. P. Wenzel, M. B. Edmond, Nosocomial bloodstream infections in US hospitals: Analysis of 24,179 cases from a prospective nationwide surveillance study. *Clin. Infect. Dis.* **39**, 309–317 (2004).
5. H. A. Khan, A. Ahmad, R. Mehboob, Nosocomial infections and their control strategies. *Asian Pac. J. Trop. Biomed.* **5**, 509–514 (2015).
6. R. T. Sadikot, T. S. Blackwell, J. W. Christman, A. S. Prince, Pathogen-host interactions in *Pseudomonas aeruginosa* pneumonia. *Am. J. Respir. Crit. Care Med.* **171**, 1209–1223 (2005).
7. M. Bassetti, A. Vena, A. Croxatto, E. Righi, B. Guery, How to manage *Pseudomonas aeruginosa* infections. *Drugs Context* **7**, 212527 (2018).
8. M. F. Moradali, S. Ghods, B. H. Rehm, *Pseudomonas aeruginosa* lifestyle: A paradigm for adaptation, survival, and persistence. *Front. Cell. Infect. Microbiol.* **7**, 39 (2017).
9. E. A. Copelan, Hematopoietic stem-cell transplantation. *N. Engl. J. Med.* **354**, 1813–1826 (2006).
10. B. R. Blazar, W. J. Murphy, M. Abedi, Advances in graft-versus-host disease biology and therapy. *Nat. Rev. Immunol.* **12**, 443–458 (2012).
11. J. Bach, Immunosuppressive therapy of autoimmune diseases. *Immunol. Today* **14**, 322–326 (1993).
12. I. Tabas, C. K. Glass, Anti-inflammatory therapy in chronic disease: Challenges and opportunities. *Science* **339**, 166–172 (2013).
13. D. D. Richman, HIV chemotherapy. *Nature* **410**, 995–1001 (2001).
14. L. Zitvogel, L. Apetoh, F. Ghiringhelli, G. Kroemer, Immunological aspects of cancer chemotherapy. *Nat. Rev. Immunol.* **8**, 59–73 (2008).
15. J. R. Quesada, M. Talpaz, A. Rios, R. Kurzrock, J. U. Gutterman, Clinical toxicity of interferons in cancer patients: A review. *J. Clin. Oncol.* **4**, 234–243 (1986).
16. E. V. Granowitz, R. B. Brown, Antibiotic adverse reactions and drug interactions. *Crit. Care Clin.* **24**, 421–442 (2008).
17. M. L. Hoffman-Terry, H. S. Fraimow, T. R. Fox, B. G. Swift, J. E. Wolf, Adverse effects of outpatient parenteral antibiotic therapy. *Am. J. Med.* **106**, 44–49 (1999).
18. K. Sedky, S. Lippmann, Psychotropic medications and leukopenia. *Curr. Drug Targets* **7**, 1191–1194 (2006).
19. R. Dholakia, S. J. Schleifer, Y. J. Ahmad, I. S. Narang, Delayed-onset mirtazapine-related leukopenia and rechallenge. *J. Clin. Psychopharmacol.* **30**, 758 (2010).
20. J. Zhou, A. V. Kroll, M. Holay, R. H. Fang, L. Zhang, Biomimetic nanotechnology toward personalized vaccines. *Adv. Mater.* **32**, 1901255 (2020).
21. Z. Guo, L. J. Kubiatowicz, R. H. Fang, L. Zhang, Nanotoxoids: Biomimetic nanoparticle vaccines against infections. *Adv. Ther.* **4**, 2100072 (2021).

22. R. H. Fang, A. V. Kroll, W. Gao, L. Zhang, Cell membrane coating nanotechnology. *Adv. Mater.* **30**, 1706759 (2018).
23. X. Wei, J. Gao, F. Wang, M. Ying, P. Angsantikul, A. V. Kroll, J. Zhou, W. Gao, W. Lu, R. H. Fang, L. Zhang, In situ capture of bacterial toxins for antivirulence vaccination. *Adv. Mater.* **29**, 1701644 (2017).
24. X. Wei, D. Ran, A. Campeau, C. Xiao, J. Zhou, D. Dehaini, Y. Jiang, A. V. Kroll, Q. Zhang, W. Gao, D. J. Gonzalez, R. H. Fang, L. Zhang, Multiantigenic nanotoxoids for antivirulence vaccination against antibiotic-resistant Gram-negative bacteria. *Nano Lett.* **19**, 4760–4769 (2019).
25. M. S. Mulani, E. E. Kamble, S. N. Kumkar, M. S. Tawre, K. R. Pardesi, Emerging strategies to combat ESKAPE pathogens in the era of antimicrobial resistance: A review. *Front. Microbiol.* **10**, 539 (2019).
26. G. V. Asokan, T. Ramadhan, E. Ahmed, H. Sanad, WHO global priority pathogens list: A bibliometric analysis of Medline-PubMed for knowledge mobilization to infection prevention and control practices in Bahrain. *Oman Med. J.* **34**, 184–193 (2019).
27. M. D. Obritsch, D. N. Fish, R. MacLaren, R. Jung, Nosocomial infections due to multidrug-resistant *Pseudomonas aeruginosa*: Epidemiology and treatment options. *Pharmacotherapy* **25**, 1353–1364 (2005).
28. N. Mesaros, P. Nordmann, P. Plesiat, M. Roussel-Delvallez, J. Van Eldere, Y. Glupczynski, Y. Van Laethem, F. Jacobs, P. Lebecque, A. Malfroot, P. M. Tulkens, F. Van Bambeke, *Pseudomonas aeruginosa*: Resistance and therapeutic options at the turn of the new millennium. *Clin. Microbiol. Infect.* **13**, 560–578 (2007).
29. Z. Pang, R. Raudonis, B. R. Glick, T. J. Lin, Z. Cheng, Antibiotic resistance in *Pseudomonas aeruginosa*: Mechanisms and alternative therapeutic strategies. *Biotechnol. Adv.* **37**, 177–192 (2019).
30. E. Sen-Kilic, C. B. Blackwood, A. B. Huckaby, A. M. Horspool, K. L. Weaver, A. C. Malkowski, W. T. Witt, J. R. Bevere, F. H. Damron, M. Barbier, Defining the mechanistic correlates of protection conferred by whole-cell vaccination against *Pseudomonas aeruginosa* acute murine pneumonia. *Infect. Immun.* **89**, e00451-20 (2021).
31. S. M. de Souza Morais, N. F. Rodigues, N. I. O. da Silva, E. A. Salvador, I. R. Franco, G. A. P. de Souza, P. H. C. da Silva, L. G. N. de Almeida, R. P. Rocha, A. C. T. da Cunha Pereira, G. P. Ferreira, P. V. Quelemes, M. P. de Araujo, F. F. Sperandio, L. J. de Souza Santos, O. A. M. Filho, L. C. C. Malaquias, L. F. L. Coelho, Serum albumin nanoparticles vaccine provides protection against a lethal *Pseudomonas aeruginosa* challenge. *Vaccine* **36**, 6408–6415 (2018).
32. Y. Wu, G. Y. Deng, Z. Y. Song, K. Zhang, J. M. Deng, K. Jiang, H. Y. Han, Enhancing antibacterial immunotherapy for bacterial pneumonia via nanovaccines coated with outer membrane vesicles. *Chem. Eng. J.* **436**, 135040 (2022).
33. Z. J. C. Gonzaga, C. Merakou, A. DiGiandomenico, G. P. Priebe, B. H. A. Rehm, A *Pseudomonas aeruginosa*-derived particulate vaccine protects against *P. aeruginosa* infection. *Vaccines* **9**, 803 (2021).
34. E. Sen-Kilic, C. B. Blackwood, D. T. Boehm, W. T. Witt, A. C. Malkowski, J. R. Bevere, T. Y. Wong, J. M. Hall, S. D. Bradford, M. E. Varney, F. H. Damron, M. Barbier, Intranasal peptide-based FpvA-KLH conjugate vaccine protects mice from *Pseudomonas aeruginosa* acute murine pneumonia. *Front. Immunol.* **10**, 2497 (2019).
35. A. Emadi, R. J. Jones, R. A. Brodsky, Cyclophosphamide and cancer: Golden anniversary. *Nat. Rev. Clin. Oncol.* **6**, 638–647 (2009).
36. L. Lin, P. Nonejuie, J. Munguia, A. Hollands, J. Olson, Q. Dam, M. Kumaraswamy, H. Rivera Jr., R. Corriden, M. Rohde, M. E. Hensler, M. D. Burkart, J. Pogliano, G. Sakoulas, V. Nizet, Azithromycin synergizes with cationic antimicrobial peptides to exert bactericidal and therapeutic activity against highly multidrug-resistant Gram-negative bacterial pathogens. *EBioMedicine* **2**, 690–698 (2015).
37. M. J. Richards, J. R. Edwards, D. H. Culver, R. P. Gaynes, Nosocomial infections in medical intensive care units in the United States. National Nosocomial Infections Surveillance System. *Crit. Care Med.* **27**, 887–892 (1999).
38. S. J. Cryz Jr., E. Furer, R. Germanier, Simple model for the study of *Pseudomonas aeruginosa* infections in leukopenic mice. *Infect. Immun.* **39**, 1067–1071 (1983).
39. J. M. Scarff, J. B. Goldberg, Vaccination against *Pseudomonas aeruginosa* pneumonia in immunocompromised mice. *Clin. Vaccine Immunol.* **15**, 367–375 (2008).
40. B. U. von Specht, B. Knapp, G. Muth, M. Broker, K. D. Hungerer, K. D. Diehl, K. Massarrat, A. Seemann, H. Domdey, Protection of immunocompromised mice against lethal infection with *Pseudomonas aeruginosa* by active or passive immunization with recombinant *P. aeruginosa* outer membrane protein F and outer membrane protein I fusion proteins. *Infect. Immun.* **63**, 1855–1862 (1995).
41. A. J. Ammann, G. Schiffman, D. Abrams, P. Volberding, J. Ziegler, M. Conant, B-cell immunodeficiency in acquired immune deficiency syndrome. *JAMA* **251**, 1447–1449 (1984).
42. A. Taddio, M. Ipp, S. Thivakaran, A. Jamal, C. Parikh, S. Smart, J. Sovran, D. Stephens, J. Katz, Survey of the prevalence of immunization non-compliance due to needle fears in children and adults. *Vaccine* **30**, 4807–4812 (2012).
43. M. R. Neutra, P. A. Kozlowski, Mucosal vaccines: The promise and the challenge. *Nat. Rev. Immunol.* **6**, 148–158 (2006).
44. C. Cao, M. Yu, Y. Chai, Pathological alteration and therapeutic implications of sepsis-induced immune cell apoptosis. *Cell Death Dis.* **10**, 782 (2019).
45. A. R. Hauser, The type III secretion system of *Pseudomonas aeruginosa*: Infection by injection. *Nat. Rev. Microbiol.* **7**, 654–665 (2009).
46. F. S. Sutterwala, L. A. Mijares, L. Li, Y. Ogura, B. I. Kazmierczak, R. A. Flavell, Immune recognition of *Pseudomonas aeruginosa* mediated by the IPAF/NLRC4 inflammasome. *J. Exp. Med.* **204**, 3235–3245 (2007).
47. C. K. Lin, B. I. Kazmierczak, Inflammation: A double-edged sword in the response to *Pseudomonas aeruginosa* infection. *J. Innate Immun.* **9**, 250–261 (2017).
48. A. Y. Koh, G. P. Priebe, G. B. Pier, Virulence of *Pseudomonas aeruginosa* in a murine model of gastrointestinal colonization and dissemination in neutropenia. *Infect. Immun.* **73**, 2262–2272 (2005).
49. K. Hubel, D. C. Dale, A. Engert, W. C. Liles, Current status of granulocyte (neutrophil) transfusion therapy for infectious diseases. *J Infect Dis* **183**, 321–328 (2001).
50. R. R. Lovewell, Y. R. Patankar, B. Berwin, Mechanisms of phagocytosis and host clearance of *Pseudomonas aeruginosa*. *Am. J. Physiol. Lung Cell. Mol. Physiol.* **306**, L591–L603 (2014).
51. M. M. Chen, J. L. Palmer, T. P. Plackett, C. R. Deburghgraeve, E. J. Kovacs, Age-related differences in the neutrophil response to pulmonary *Pseudomonas* infection. *Exp. Gerontol.* **54**, 42–46 (2014).
52. J. A. Bluestone, Mechanisms of tolerance. *Immunol. Rev.* **241**, 5–19 (2011).
53. B. T. Luk, R. H. Fang, C. M. Hu, J. A. Copp, S. Thamphiwatana, D. Dehaini, W. Gao, K. Zhang, S. Li, L. Zhang, Safe and immunocompatible nanocarriers cloaked in RBC membranes for drug delivery to treat solid tumors. *Theranostics* **6**, 1004–1011 (2016).
54. Q. Zhang, A. Honko, J. Zhou, H. Gong, S. N. Downs, J. H. Vasquez, R. H. Fang, W. Gao, A. Griffiths, L. Zhang, Cellular nanosponges inhibit SARS-CoV-2 infectivity. *Nano Lett.* **20**, 5570–5574 (2020).
55. C. M. Hu, R. H. Fang, K. C. Wang, B. T. Luk, S. Thamphiwatana, D. Dehaini, P. Nguyen, P. Angsantikul, C. H. Wen, A. V. Kroll, C. Carpenter, M. Ramesh, V. Qu, S. H. Patel, J. Zhu, W. Shi, F. M. Hofman, T. C. Chen, W. Gao, K. Zhang, S. Chien, L. Zhang, Nanoparticle biointerfacing by platelet membrane cloaking. *Nature* **526**, 118–121 (2015).
56. A. V. Kroll, R. H. Fang, Y. Jiang, J. Zhou, X. Wei, C. L. Yu, J. Gao, B. T. Luk, D. Dehaini, W. Gao, L. Zhang, Nanoparticulate delivery of cancer cell membrane elicits multiantigenic antitumor immunity. *Adv. Mater.* **29**, 1703969 (2017).
57. Y. Jiang, N. Krishnan, J. Zhou, S. Chekuri, X. Wei, A. V. Kroll, C. L. Yu, Y. Duan, W. Gao, R. H. Fang, L. Zhang, Engineered cell-membrane-coated nanoparticles directly present tumor antigens to promote anticancer immunity. *Adv. Mater.* **32**, 2001808 (2020).
58. Q. Zhang, D. Dehaini, Y. Zhang, J. Zhou, X. Chen, L. Zhang, R. H. Fang, W. Gao, L. Zhang, Neutrophil membrane-coated nanoparticles inhibit synovial inflammation and alleviate joint damage in inflammatory arthritis. *Nat. Nanotechnol.* **13**, 1182–1190 (2018).

Acknowledgments

Funding: This work was supported by Defense Threat Reduction Agency Joint Science and Technology Office for Chemical and Biological Defense grant HDTRA1-18-1-0014 (L.Z.) and National Institutes of Health grant R21AI159492 (R.H.F.). **Author contributions:** J.Z., R.H.F., and L.Z. conceived and designed the experiments. J.Z. conducted all experiments. N.K. and Z.G. assisted with the pneumonia experiments. C.J.V. supported the in vitro assays. N.K., Z.G., and M.H. helped with the septicemia studies. Q.Z. developed the primary neutrophil derivation process. All authors analyzed and discussed the data. J.Z., R.H.F., and L.Z. interpreted the data and wrote the paper. **Competing interests:** The authors declare that they have no competing interests. **Data and materials availability:** All data needed to evaluate the conclusions in the paper are present in the paper and/or the Supplementary Materials.

Submitted 15 April 2022
Accepted 22 July 2022
Published 9 September 2022
10.1126/sciadv.abq5492